Suppression of dopamine receptor 2 inhibits the formation of human prostate cancer PC-3-derived cancer stem cell-like cells through AMPK inhibition

JUYEON PARK[1*], HEE JUN JANG[1*], WON KI JUNG[1*], DA YEON KANG[1], YOU LI GONG[1], HEE-JEONG KIM[1], JONG SOON KANG[2], JEONG WOOK YANG[2], YOUNGJOO BYUN[1,3] and SONG-KYU PARK[1,3]

[1]College of Pharmacy, Korea University, Sejong 30019, Republic of Korea; [2]Laboratory Animal Resource Center, Korea Research Institute of Bioscience and Biotechnology, Cheongju, Chungbuk 28116, Republic of Korea; [3]Biomedical Research Center of Guro Hoipital, Research-Driven Hospital, Korea University, Seoul 08308, Republic of Korea

Received October 10, 2024; Accepted January 2, 2025

DOI: 10.3892/ol.2025.14888

Abstract. Cancer stem cells (CSCs) contribute to the resistance of intractable prostate cancer, and dopamine receptor (DR)D2 antagonists exhibit anticancer activity against prostate cancer and CSCs. Human prostate cancer PC-3 cells were used to generate CSC-like cells, serving as a surrogate system to identify the specific DR subtype the inhibition of which significantly affects prostate-derived CSCs. Additionally, the present study aimed to determine the downstream signaling molecules of this DR subtype that exert more profound effects compared with other DR subtypes. The inhibitory effects of specific antagonists or small interfering (si)RNAs on DR subtypes were compared by analyzing morphological changes of cells, expression patterns of pluripotency markers, cell growth inhibitory activities and *in vitro* cell invasion. L-741,626, a specific DRD2 antagonist, induced morphological changes in PC-3-derived CSC-like cells, suppressed the expression of Oct4 (a pluripotency marker), and inhibited the growth of cells and tumors. The proliferation of heterozygous null PC-3 cells, generated using the CRISPR/Cas9 method, was slow, and their sphere-forming ability was substantially reduced, indicating a diminished capacity to produce CSCs. In addition, the phosphorylation of AMPK was suppressed by DRD2 siRNA and the heterozygous knockout of DRD2 in PC-3 cells, indicating that AMPK may be a putative downstream signaling molecule involved in the production and maintenance of PC-3-derived CSC-like cells. Specific inhibition or suppression of DRD2 caused PC-3-derived CSC-like cells to lose their properties and inhibited the formation of PC-3-derived CSC-like cells, followed by inhibition of the phosphorylation of AMPK, which is considered a putative downstream signaling molecule of DRD2. Further understanding of the mechanisms by which DRD2 regulates AMPK and the effects of AMPK inhibition on the properties of PC-3-derived CSC-like cells may provide valuable insights into the identification of molecular targets for treating intractable prostate cancer wherein AMPK is constitutively activated.

Correspondence to: Dr Song-Kyu Park or Dr Youngjoo Byun, College of Pharmacy, Korea University, 2511 Sejong-ro, Sejong 30019, Republic of Korea
E-mail: spark123@korea.ac.kr
E-mail: yjbyun1@korea.ac.kr

*Contributed equally

Key words: dopamine receptors, PC-3 cells, cancer stem cells, prostate cancer, AMPK

Introduction

Prostate cancer incidence is considerably high in Western and developed Asian countries. Although the 5-year survival rate of prostate cancer is ~97%, which is one of the highest among cancers, mortality due to prostate cancer is substantilly high, ranking it second among all cancer-related deaths (1). Chemotherapeutic agents such as docetaxel and cabazitaxel and androgen signaling inhibitors such as abiraterone and enzalutamide have successfully been used to treat prostate cancer. However, the recurrence of prostate cancer resistant to these therapies, such as castration-resistant prostate cancer (CRPC), and the side effects of these therapies, which includes impotence, continue to affect the quality of life of patients (2,3).

Although safe and effective methods for treating prostate cancer are being investigated, effective androgen-independent therapies for advanced prostate cancer remain unavailable. Similar to other tumor types, a very small proportion (<1%) of cancer stem cells (CSCs) are present in prostate cancer (4,5). Prostate CSCs differentiate into androgen-dependent and androgen-independent carcinomas. Androgen-independent carcinomas are more resistant to anticancer therapy. Thus, in addition to conventional chemotherapy, novel therapies targeting CSCs are required to prevent CSCs from continuously supplying androgen-independent carcinomas. Accordingly, it is necessary to elucidate the characteristics of prostate CSCs and identify methods to mitigate their properties to effectively treat patients with CRPC (6,7).

Because the elimination of CSCs in various tumor types using conventional anticancer agents has been ineffective, the differentiation of CSCs into nonmalignant cells has been attempted for different cancer types (8-10). Previous studies on other cancer types have reported the use of differentiation therapy to convert prostate CSCs into more differentiated cells (11). However, these studies were unsuccessful. Further understanding of signal transduction involved in the differentiation of prostate CSCs can help develop anticancer therapies, including differentiation therapies. ZEP1, YAP1, and TMPRSS4, which are involved in maintaining the properties of prostate CSCs, are potential targets for the differentiation therapy of prostate cancer (12-14).

Previous studies have suggested the use of dopamine receptor 2 (DRD2) antagonists as putative anticancer agents (15,16). Neoplastic human pluripotent stem cells (hPSCs) possessing CSC-like properties were differentiated into cells that lost their pluripotency due to treatment with dopamine receptor (DR) antagonists, such as thioridazine (10). Our previous study using CSC-like cells derived from PC-3 cell lines (human prostate cancer cells) and thiordazine yielded results very similar to those obtained using the hPSCs described above (17). In addition, our previous study suggested that thioridazine induces the differentiation of PC-3-derived CSC-like cells via AMPK inhibition. However, thioridazine inhibits other types of receptors, including histamine, muscarine, and serotonin receptors, in addition to DRD2 (18-20). Accordingly, it must be clarified that the differentiation of PC-3-derived CSC-like cells using thioridazine was induced by DRD2 inhibition and not by the nonspecific inhibition of different receptors. Herein, PC-3-derived CSC-like cells were transfected with siRNA or treated with highly specific antagonists against five different DR subtypes (DRD1-DRD5) and the effects of the inhibition of each receptor subtype were compared. In addition, the involvement of DRD2 in the formation of PC-3-derived CSC-like cells was confirmed using the heterozygous knockout of the DRD2 gene in PC-3 cells via the CRISPR/Cas9 method and by investigating the effects of DRD2 knockdown in the cells.

Materials and methods

Reagents. LE300, L-741,626, PG 01037, PD 168568, and SCH 39166 were purchased from Tocris. Antibodies against Akt, phosphor-Akt, AMPKa, phospho-AMPKa, mTOR, phospho-mTOR, SAPK/JNK, phospho-SAPK/JNK, Oct4, Klf4, c-Myc, and b-actin were purchased from Cell Signaling Technology. Unless otherwise stated, all other reagents were purchased from Merck KGaA.

Cell lines. The human prostate cancer cell line PC-3 was obtained from the American Type Culture Collection and cultured in RPMI-1640 medium supplemented with 10% (v/v) heat-inactivated fetal bovine serum (FBS). Cell cultures enriched for CSC-like cells derived from PC-3 cells were prepared according to a previously described protocol (17). Briefly, PC-3 cells were trypsinized, harvested after washing with phosphate-buffered saline (PBS), and then suspended in serum-free DMEM/F12 medium (R&D Systems) supplemented with 100 IU/ml penicillin, 100 μg/ml streptomycin, 10 ng/ml human recombinant epidermal growth factor (hrEGF; R&D Systems), 10 ng/ml human recombinant basic fibroblast growth factor (hrbFGF; R&D Systems), and 2% B27 supplement (Thermo Fisher Scientific, Inc.). These suspended cells were cultured in ultralow attachment culture dishes at a density of $1x10^6$ cells/dish and then allowed to form tumorspheres for 7 days. Single cells obtained via the trypsinization of the tumorspheres were collected and allowed to form an adherent monolayer culture in a regular animal cell culture ware in the abovementioned serum-free medium and maintained in serum-free DMEM/F12 medium supplemented with 100 IU/ml penicillin, 100 μg/ml streptomycin, 10 ng/ml hrEGF, 10 ng/ml hrbFGF, and 2% B27 supplement.

Immunocytochemistry. The cells were seeded into a four-chamber plate (Falcon) at a density of $1x10^4$ cells/well, incubated for 72 h, and fixed with 3.7% formaldehyde at room temperature for 10 min. Fixed cells were permeabilized with 0.1% Tween-20 in PBS (pH 7.4) for 5 min, blocked with PBS containing 1% bovine serum albumin (BSA) for 30 min, and incubated with a rabbit monoclonal antibody against DRD1, DRD2, DRD3, DRD4, and DRD5 at 4˚C overnight. The cells were washed with PBS and incubated in the presence of goat antirabbit IgG conjugated with Alexa Fluor™ 594 (Thermo Fisher Scientific, Inc.) for 1 h in the dark. Alexa Fluor™ 488 Phalloidin (Thermo Fisher Scientific, Inc.) diluted to a ratio of 1:40 using PBS was added to the wells and incubated for another 20 min. The cells were washed with PBS, stained with DAPI for 5 min, and observed under an LSM 700 confocal microscope (Zeiss).

Human tumor xenografts in nude mice. The Institutional Animal Care & Use Committee (IACUC) of Korea University (Seoul, Korea), reviewed and approved the animal study protocol (protocol number: KUIACUC-2021-0028). Six- to seven-week-old female Balb/c nude mice (Charles River Laboratories) were maintained as previously described (21). Cancer cells ($5x10^6$ cells/200 μl/mouse) suspended in PBS (pH 7.4) were injected subcutaneously into the right flank of a mice. Tumor volumes were measured 2-3 times weekly using a Vernier caliper and were calculated using the following equation: Tumor volume=$Dmin^2$ x Dmax x 0.5 (Dmin: short axis, Dmax: long axis of mass). The experiments were stopped before the tumor volume reached 1,000 mm^3 and the mice were euthanized by introducing CO_2 into the euthanasia chamber at a rate sufficient to fill 50% of the chamber's volume per minute. The mice were continuously monitored for visible signs of death, such as cessation of breathing and lack of movement. Even after observing the visible signs of death, CO_2 exposure were continued for an additional 1 min. After then, the tumors were collected from the mice.

siRNA transfection. PC-3-derived CSC-like cells were seeded into tissue culture plates at a density of $3x10^4$ to $1x10^5$ cells/ml depending on the type of experiment using antibiotic-free DMEM/F12 medium with supplements and growth factors. To silence the expression of the DRD subtype genes, the cells were transfected for 6 h with 50-100 pmol/ml of control siRNA and DRD1, DRD2, DRD3, DRD4, and DRD5 siRNA separately using the siRNA Reagent System

(Santa Cruz Biotechnology, Inc.) following the manufacturer's instructions (see Table SI for more information about siRNA).

Semiquantitative reverse transcription (RT)-polymerase chain reaction (PCR). Total RNA was extracted from cells using a GeneAll kit (GeneAll Biotechnology), and cDNA was prepared and amplified using a One Step RT-PCR kit (SolGent). Table SII shows the primer sequences for the dopamine receptor subtypes (DRD1, DRD2, DRD3, DRD4, and DRD5) and GAPDH. The PCR products were subjected to electrophoresis using 1.5-1.8% agarose gel and visualized after staining with ethidium bromide.

cAMP assay. PC-3-derived CSC-like cells were transfected with siRNA against DRD1-DRD5 and seeded in 96-well plates at a density of $5x10^4$ cells/well. After 24 h of incubation, the intracellular cAMP levels were assayed using cAMP-Glo™ assay (Promega) following the manufacturer's instructions. Luminescence was measured using a Centro LB 960 microplate luminometer (Berthold Technologies).

Cell growth assay. To measure the growth of PC-3-derived CSC-like cells transfected with DRD siRNAs, the WST-8 assay (Biomax) was used. Briefly, 24 h after seeding the cells in a six-well culture plate at a density of $1x10^4$ cells/ml, WST-8 assay was conducted at designated times and absorbance was measured at 450 nm. To determine the growth of DRD2 heterozygous knockout PC-3 cells, the cells were seeded into a six-well culture plate at a density of $1x10^4$ cells/ml and grown in RPMI-1640 medium supplemented with 10% heat-inactivated FBS at 37˚C. The cells were trypsinized and harvested at designated times and counted using an automated cell counter (Countess™ II #AMQX1000).

In vitro cell invasion assay. The insert polycarbonate membranes (8 mm in pore size) of the upper compartments of the 24-well Transwell Boyden chamber were coated with Matrigel® (BD Biosciences) diluted using a serum-free medium. Depending on the cell type, 300 μl of cells ($1.5x10^5$ cells/ml) suspended in RPMI-1640 or DMEM/F12 medium were placed in the upper compartment. The lower compartment was then filled with 500 μl of RPMI-1640 medium supplemented with 10% FBS or serum-free DMEM/F12 medium supplemented with 2% B-27 supplements and growth factors. The cells on the lower side of the insert membrane were fixed with 10% trichloroacetic acid (TCA) and stained with 0.5% crystal violet in 2% ethanol for 2 h. The insert was washed with PBS and air dried. The upper side of the insert was wiped using a cotton swab, and images of the cells that had migrated to the underside of the insert membrane were taken. The dye that stained the cells was extracted with 0.2 ml of 30% acetic acid, and the absorbance was measured at 590 nm.

Western blotting analysis. Protein extracts (20 μg) of cell lysates were resolved on 8-10% SDS-polyacrylamide gels and transferred to Immobilon-P transfer membranes as described previously (22). The membranes were blocked with Tris-buffered saline containing 0.1% Tween-20 (TBST) supplemented with 0.5-2% BSA and probed with primary antibodies. After washing with TBST, the membranes were probed with species-specific horseradish peroxidase (HRP)-conjugated secondary antibodies and developed using an Immobilon western chemiluminescent HRP substrate.

Staining of cells to observe morphological changes. The cells incubated for 6 days in the presence and absence of compounds were fixed with 50% TCA and stained with 0.4% sulforhodamine B (SRB) in 0.1% acetic acid. Excess staining was removed by washing the cells with 1% acetic acid. The morphology of the stained cells was observed using an inverted microscope and photographed (Nikon).

Preparation of DRD2 heterozygous knockout ($DRD2^{+/-}$) PC-3 cells. PC-3 cells were seeded into 60-mm dishes at a density of $1.5x10^5$ cells/ml and cultured in an antibiotic-free medium. When the cells were at ~80% confluency, they were transfected with an all-in-one vector (Macrogen, Seoul, Korea) containing the DRD2 sgRNA sequence (5'-GGTATGATGATGATCTGG AGAGG-3'), puromycin resistance gene, and CAS9 expression gene using the *Trans*IT-LT1 transfection reagent (Mirus Bio) following the manufacturer's instructions (see Fig. S1 for the all-in-one vector map). After 48 h, the cells were cultured on RPMI medium supplemented with 100 IU/ml penicillin, 100 μg/ml streptomycin, and 1 μg/ml puromycin for 6 days. During this period, the medium was changed daily. The surviving cells were amplified, and genomic DNA was isolated using Exgene™ Cell SV mini kit (GeneAll Biotechnology, Seoul, Korea). DNA fragments were then amplified by PCR with the DRD2 primers used in the T7 endonuclease assay and sequenced using the Sanger sequencing method (Cosmogenetech) (See the DNA sequences in Fig. S2).

T7 endonuclease assay. To validate DRD2 heterozygous knockout in PC-3 cells, genomic DNA isolated from wild-type and all-in-one vector-transfected PC-3 cells were amplified using PCR with the DRD2 primers (forward: 5'-TGTGTT TGCTCATTTGTCCTACC-3', reverse: 5'-AGGAAACAA TCTACCCATTTCGT-3'). The amplified DNA products were incubated at 37˚C for 20 min in the presence of T7 endonuclease (Goldbio). The reaction products were then subjected to electrophoresis using 1.2% agarose gel and visualized after staining with ethidium bromide.

Sphere formation assay. Wild-type, mock-transfected, and $DRD2^{+/-}$ PC-3 cells grown in RPMI medium containing 10% heat-inactivated FBS were trypsinized and cultured at a density of $1x10^4$ cells/well in an ultralow attachment six-well plate containing DMEM/F12 medium supplemented with 2% B27, 10 ng/ml hrEGF, and 10 ng/ml hrbFGF. Round cell clusters of >40 μm were classified as spheres.

Statistical analysis. GraphPad Prism 5.03 (GraphPad Software, Boston, Massachusetts, USA) was used for all statistical analyses. Statistical differences among experimental groups were analyzed using a unpaired Student's t-test or one-way/two-way ANOVA with Dunnett's post hoc analysis. $P<0.05$ was considered to indicate a statistically significant difference.

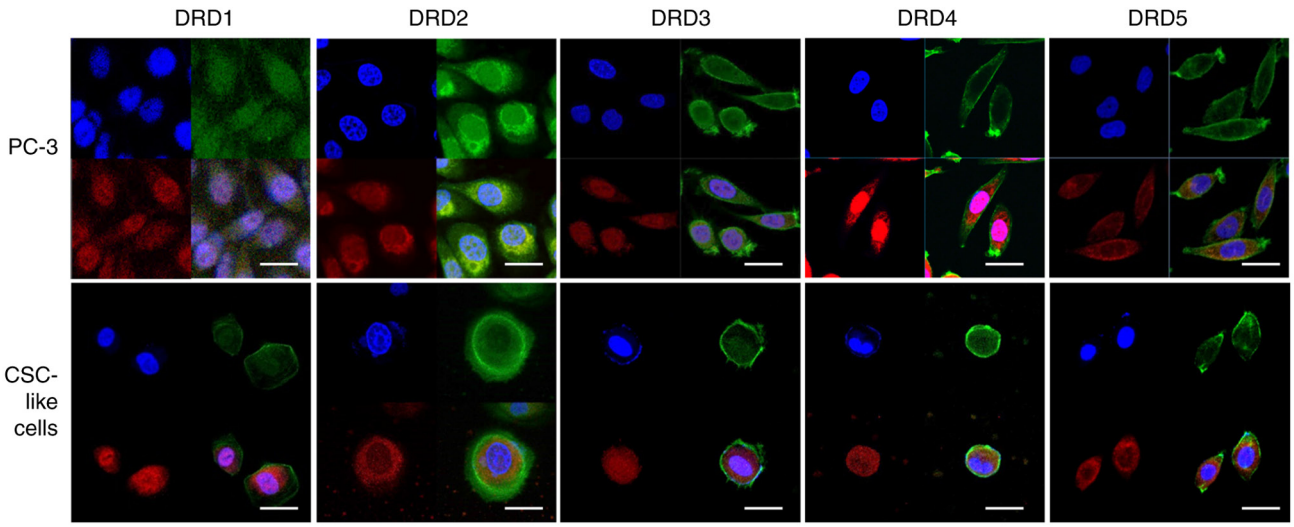

Figure 1. Intracellular location of dopamine receptor subtypes in PC-3 and PC-3-derived CSC-like cells. Cells were fixed, permeabilized, and stained as described in the Materials and Methods section. Blue: nucleus, green: F-actin, red: dopamine receptor subtype. Scale bar: 50 μm. DRD, dopamine receptor; CSC, cancer stem cell.

Results

Detection of DR subtype receptors in PC-3 and PC-3-derived CSC-like cells via immunocytochemistry. Our previous study showed that cell cultures prepared for enriching CSC-like cells from PC-3 cells possessed several properties characteristic of CSC-like cells, such as the expression of Oct4, Klf4, and Sox2. These PC-3-derived CSC-like cells were more resistant to some agents with anticancer activity such as dasatinib and saracatinib, tyrosine kinase inhibitors, and tirbanibulin, a tubulin polymerization inhibitor, than PC-3 cells (Fig. S3). In addition, the mRNA of all DR subtypes, which were of primary interest in our study, were expressed in PC-3 cells and PC-3-derived CSC-like cells (17). Immunocytochemical analysis revealed that the proteins of the DR subtypes were also expressed in these cells (Fig. 1). Capturing stained images of DRD3 was challenging, as expected from the extremely low expression of its mRNA; however, the presence of all five subtypes was detected in both the cell types.

Morphological changes and loss of pluripotency markers in PC-3-derived CSC-like cells caused by a specific DRD2 antagonist. Thioridazine used in our previous study (17) is a DRD2 antagonist but it also binds and inhibits various other receptors, including serotonin and cholinergic receptors. Thus, more specific antagonists against each DR subtype, such as LE300, L-741,626, PG 01037, PD 168568, and SCH39166, were applied to PC-3-derived CSC-like cells at a concentration of 3 μM. Subsequently, the morphological changes of the cells and the expression of pluripotency markers such as Oct4, Klf4, and c-Myc were analyzed (Fig. 2). L-742,626, a DRD2 antagonist, strongly induced morphological changes in the cells, a strong decrease in Oct4 and Klf4 protein expression, and a strong increase in c-Myc protein expression, indicating the loss of CSC properties. These results are consistent with those of our previous study (17). Meanwhile, PD 168568, a DRD4 antagonist, also induced changes in the morphology and Oct4, Klf4, and c-Myc protein expression in the cells, although the effects were weaker than those induced by L0741,626. PG-01037 induced very weak morphological changes in the cells and a slight decrease in Oct4 protein expression; however, further studies are needed to determine whether DRD2 is involved in maintaining the properties of PC-3-derived CSC-like cells.

Inhibition of the growth of tumors induced by PC-3-derived CSC-like cells by a specific DRD2 antagonist. To determine whether a specific DRD2 antagonist inhibits tumor growth *in vivo*, L-741,626 (20 mg/kg) was administered intraperitoneally to nude mice with tumors formed from PC-3-derived CSC-like cells daily. L-741,626 induced 59.5% tumor growth inhibition compared with the control group without significant changes in body weight (Fig. 3).

Downregulation of the mRNA expression of DR subtypes through transfection with siRNA against each subtype. Because the inhibition of DRD2 in PC-3-derived CSC-like cells by thioridazine, a DRD2 antagonist, appeared to induce a loss of CSC characteristics in our previous study (17), it was necessary to determine whether this effect could be mimicked by the knockdown of any DR subtype. siRNA against all five subtypes was transfected into PC-3-derived CSC-like cells. Semiquantitative RT-PCR revealed that the mRNA of each subtype was effectively downregulated by its corresponding siRNA (Fig. 4).

Effects of DR siRNA transfection on the intracellular cAMP concentration. While DRD2, DRD3, and DRD4 are type II dopamine receptors coupled to the Gs protein, DRD1 and DRD5 are type I dopamine receptors coupled to the G_i protein (23). To determine whether the siRNA-mediated knockdown of DR subtypes is functionally effective, intracellular cAMP concentrations were measured (Fig. 5). The knockdown of type I dopamine receptors suppressed intracellular cAMP concentrations to the control levels, whereas the knockdown of type II dopamine receptors increased intracellular cAMP concentrations.

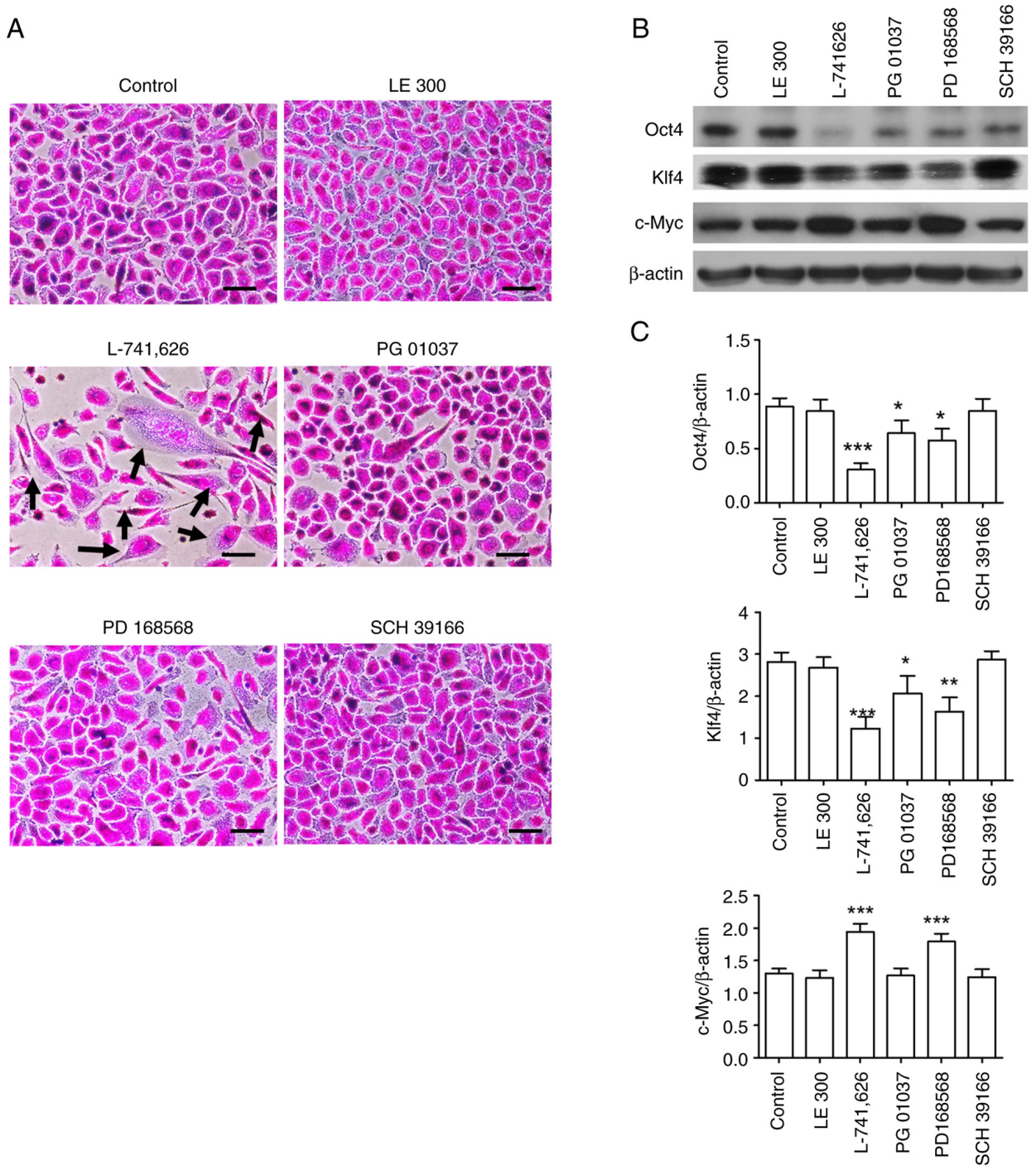

Figure 2. Effects of DR subtype antagonists on the morphology and expression of pluripotency markers in PC-3-derived CSC-like cells. (A) PC-3-derived CSC-like cells were incubated in the presence and absence of 3 μM of antagonists against DR subtypes (LE 300, L-741,626, PG 01037, PD 168568, and SCH 39166 for DRD1, DRD2, DRD3, DRD4, and DRD5, respectively) for 6 days and stained with 0.4% SRB. Black arrows indicate cells with altered morphology. Scale bar: 100 μm. (B) Lysates of cells incubated as described in (A) were subjected to western blotting. (C) Band densities of western blot images (n=3) were measured using ImageJ software. Data are presented as mean ± SD. *P<0.05, **P<0.01, ***P<0.001 vs. control. DRD, dopamine receptor; CSC, cancer stem cell.

Alteration of growth and in vitro invasion of PC-3-derived CSC-like cells by DR siRNAs. The growth of PC-3-derived CSC-like cells transfected with DRD2 siRNA decreased substantially with time (Fig. 6). Transfection with DRD4 siRNA also inhibited cell growth, but the effect was less pronounced than that caused by DRD2 siRNA. A slight but statistically significant increase in the growth of cells transfected with DRD1 or DRD3 on day 6 was observed. In contrast to the effects on cell growth, *in vitro* cell invasion remained unaffected by DRD1 and DRD3 siRNA (Fig. 7). However, it was substantially inhibited by DRD2 siRNA and slightly by DRD4 siRNA.

Inhibition of AMPK phosphorylation by DRD2 siRNA. Our previous study showed that AMPK phosphorylation was inhibited by thioridazine, a DRD2 antagonist (17). To examine whether AMPK phosphorylation is inhibited by DR knockdown, PC-3-derived CSC-like cells were transfected with DR

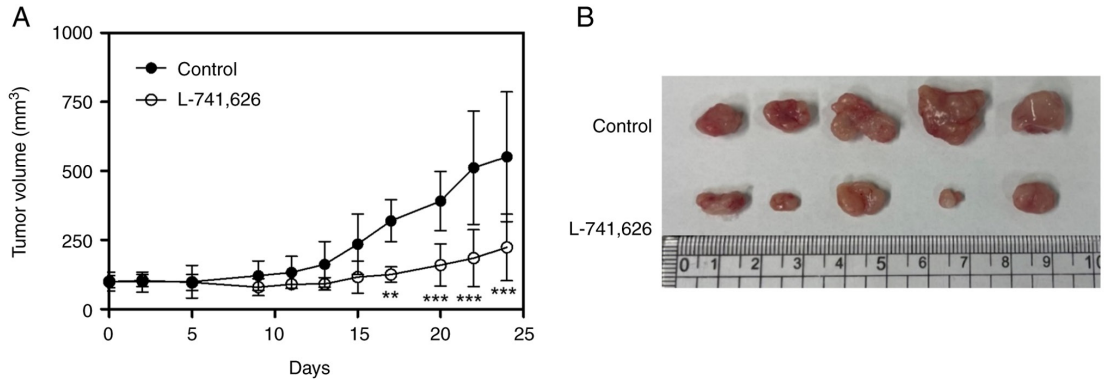

Figure 3. DRD2 antagonist inhibits the growth of tumors formed from PC-3-derived CSC-like cells. PC-3-derived CSC-like cells were transplanted subcutaneously into nude mice, and after waiting for 6 days until the average tumor volume reached ~80 mm^3, L-741,626 626 dissolved in a solvent of 5% ethanol, 5% Tween 80, and 90% saline was administered intraperitoneally at a dose of 20 mg/kg every day for 24 days. (A) Tumor volumes were measured at designated time points. (B) Tumors were collected at the end of the experiment. Data are presented as mean ± SD (n=5). **P<0.01, ***P<0.001 vs. control. DRD, dopamine receptor; CSC, cancer stem cell.

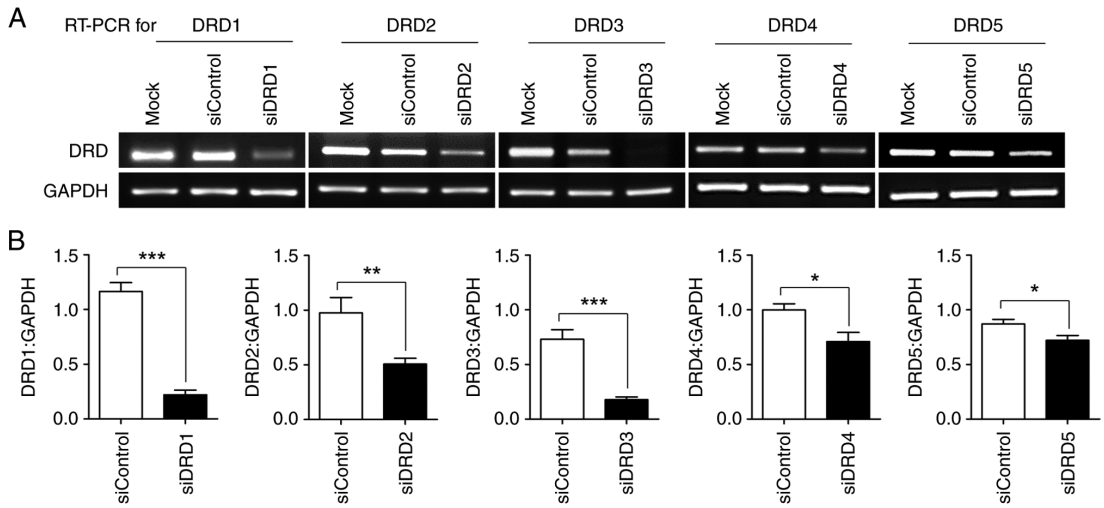

Figure 4. Downregulation of mRNA expression of dopamine receptor subtypes in PC-3-derived CSC-like cells by siRNA. (A) Twenty hours after seeding into a six-well plate at a density of $1x10^4$ cells/ml, PC-3-derived CSC-like cells were transfected with 50 pmol of each siRNA for 6 h as described in the Materials and Methods section, incubated for 48 h in the presence of fresh serum-free medium, and harvested for semiquantitative RT-PCR. (B) Band densities of RT-PCR blot images (n=3) were measured using ImageJ software. Data are presented as mean ± SD. *P<0.05, **P<0.01, ***P<0.001. DRD, dopamine receptor; GAPDH, glyceraldehyde 3-phosphate dehydrogenase; CSC, cancer stem cell; si, small interfering.

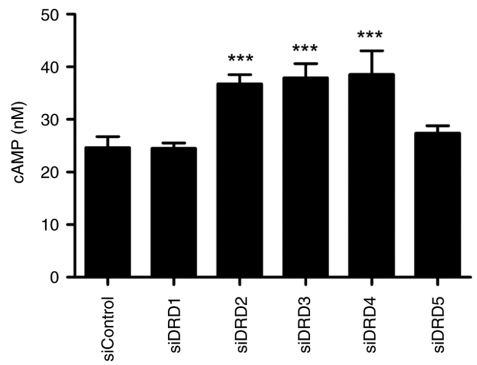

Figure 5. Effects of silencing DR expression on cAMP concentration in PC-3-derived CSC-like cells. Twenty hours after transfection with DRD siRNA, PC-3-derived CSC-like cells were seeded into a 96-well plate at a density of $5x10^4$ cells/ml and then subjected to the cAMP assay as described in the Materials and Methods section. Data are presented as mean ± SD (n=3). ***P<0.001 vs. siControl. DRD, dopamine receptor; CSC, cancer stem cell; si, small interfering.

siRNAs. Fig. 8 shows that only DRD2 siRNA significantly inhibited AMPK phosphorylation. mTOR phosphorylation, which was unaffected by thioridazine, was also unaffected by transfection with siRNA against DR subtypes.

Changes in the properties of PC-3-derived CSC-like cells after DRD2 knockdown. Because the suppression of DRD2 activity or expression with a DRD2 antagonist or siRNA changed the characteristics of PC-3-derived CSC-like cells, it was necessary to investigate whether the suppression of DRD2 expression in parental PC-3 cells affected their intrinsic characteristics, such as sphere formation ability. DRD2 heterozygous knockout ($DRD2^{+/-}$) PC-3 cells were prepared, and the heterozygotic genetic mutation was validated using the T7 endonuclease digestion method (Fig. 9A). The downregulation of DRD2 expression was observed (Fig. 9B and C). The growth of $DRD2^{+/-}$ PC-3 cells was substantially slower than that of mock-transfected PC-3 cells. Addition of 30 μM of A769662, an AMPK activator, to

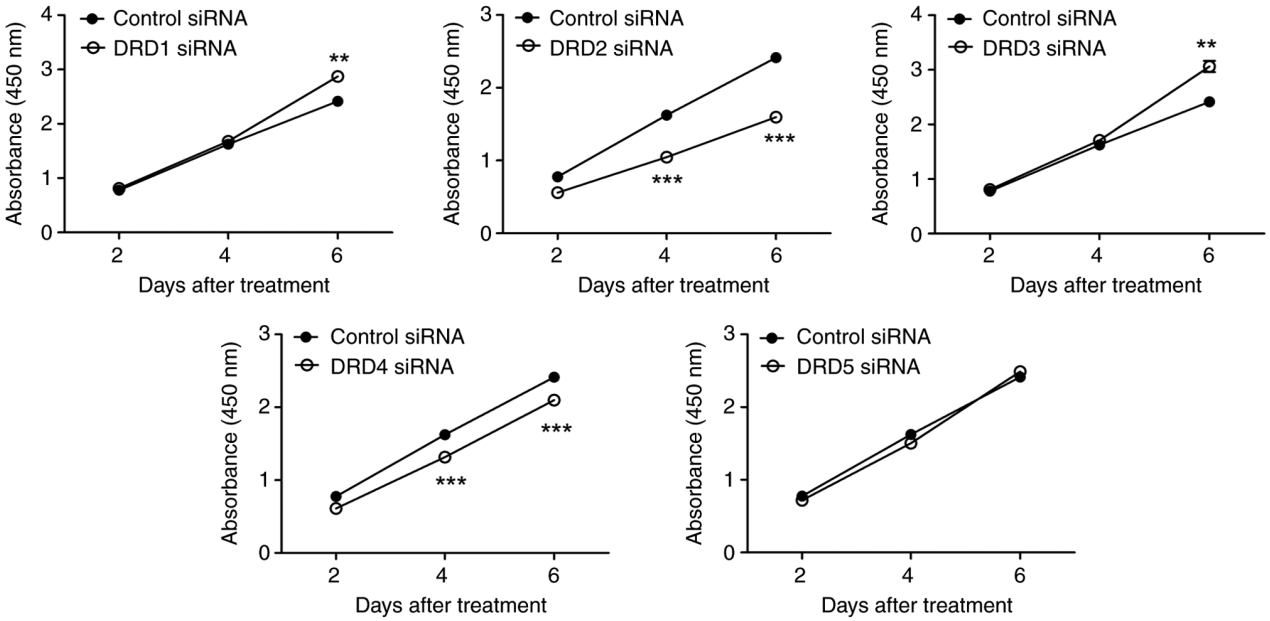

Figure 6. Effects of silencing DR expression on the growth of PC-3-derived CSC-like cells. PC-3-derived CSC-like cells were transfected for 6 h with DR siRNA and seeded into a 96-well plate at a density of $1x10^4$ cells/ml. Cells were allowed to grow and subjected to the WST-8 assay on days 2, 4, and 6. Data are presented as mean ± SD (n=4). **P<0.01, ***P<0.001 vs. siControl. DRD, dopamine receptor; CSC, cancer stem cell; si, small interfering.

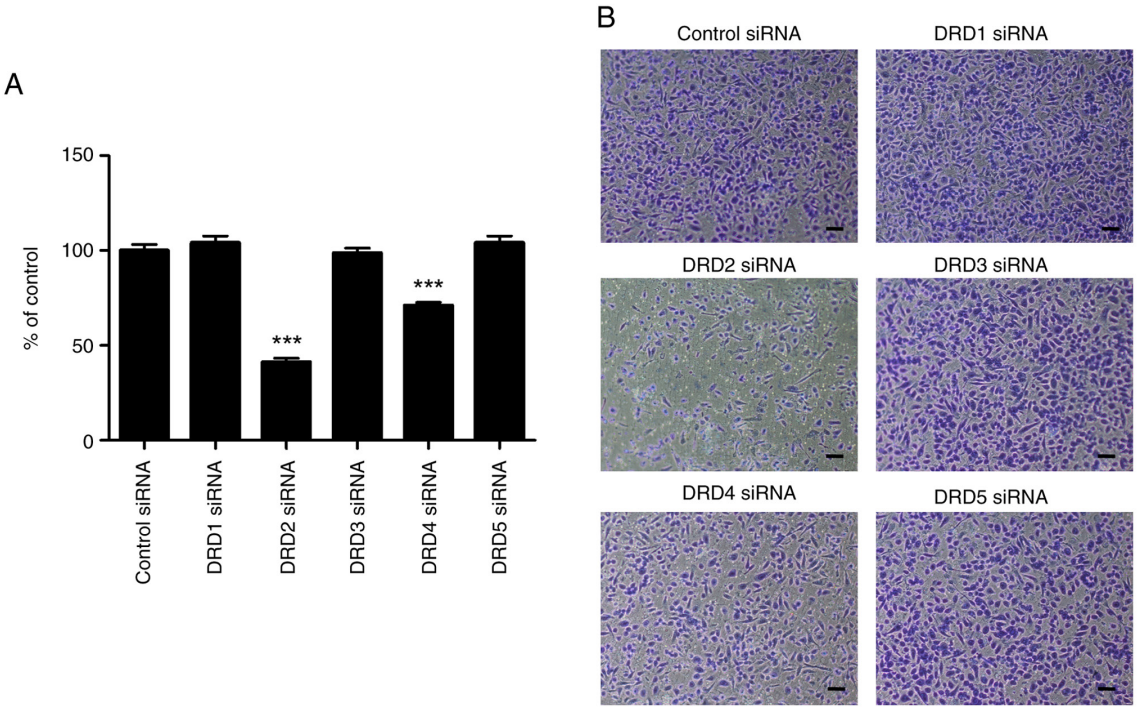

Figure 7. Effects of silencing DR expression on *in vitro* invasion of PC-3-derived CSC-like cells. (A) PC-3-derived CSC-like cells were transfected with DR siRNA, applied to the polycarbonate membranes of the upper compartments of a 24-well Transwell Boyden chamber, and allowed to invade the opposite side of the membranes for 36 h. The invaded cells were stained as described in the Materials and Methods section. The dye was extracted from the cells, and absorbance was measured at 590 nm. Data are presented as mean ± SD (n=4). ***P<0.001 vs. siControl. (B) Representative images of invaded and stained cells are shown. Scale bar: 100 μm. DRD, dopamine receptor; CSC, cancer stem cell; si, small interfering.

DRD2$^{+/-}$ PC-3 cells partially restored the cell growth (Fig. 9D). The concentration of 30 mM was chosen from the previous study as it showed the highest effects in restoring cell growth (17). The morphology of the DRD2$^{+/-}$ PC-3 cells differed substantially from that of the mock-transfected PC-3 cells (Fig. 9E). The sphere formation assay, an *in vitro* method for amplifying and isolating CSCs, revealed that the sphere-forming ability of the DRD2$^{+/-}$ PC-3 cells was substantially lower than that of the parental and mock-transfected PC-3 cells (Fig. 9F and G). Because AMPK phosphorylation in PC-3-derived CSC-like cells is inhibited by DRD2 siRNA, the effect of heterozygous DRD2 knockout on the phosphorylation of several signal

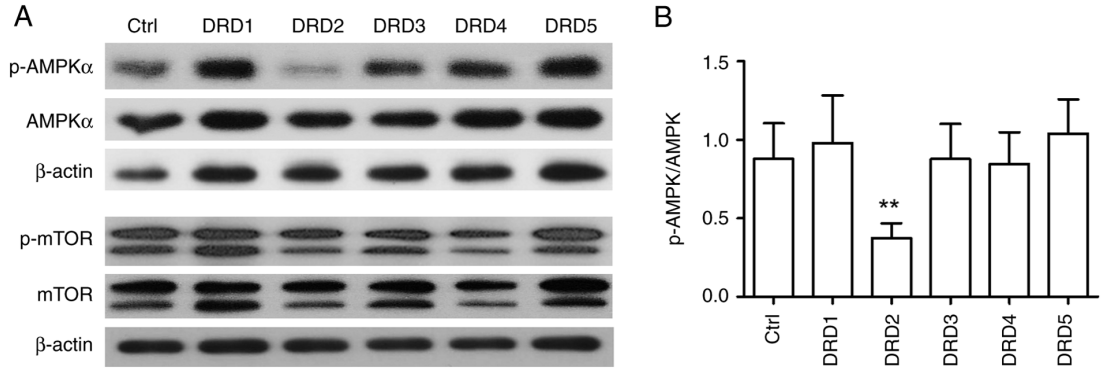

Figure 8. Inhibition of AMPK phosphorylation via suppression of DRD2 expression. (A) PC-3-derived CSC-like cells were transfected twice (day 1 and 3) with each DR siRNA 60 pmol/ml), harvested on day 7, and subjected to western blotting. (B) Band densities of western blot images (n=3) were measured using ImageJ software. Data are presented as mean ± SD. **P<0.01 vs. Ctrl. Ctrl, control; DRD, dopamine receptor; AMPK, 5' AMP-activated protein kinase; mTOR, mammalian target of rapamycin; CSC, cancer stem cell; si, small interfering.

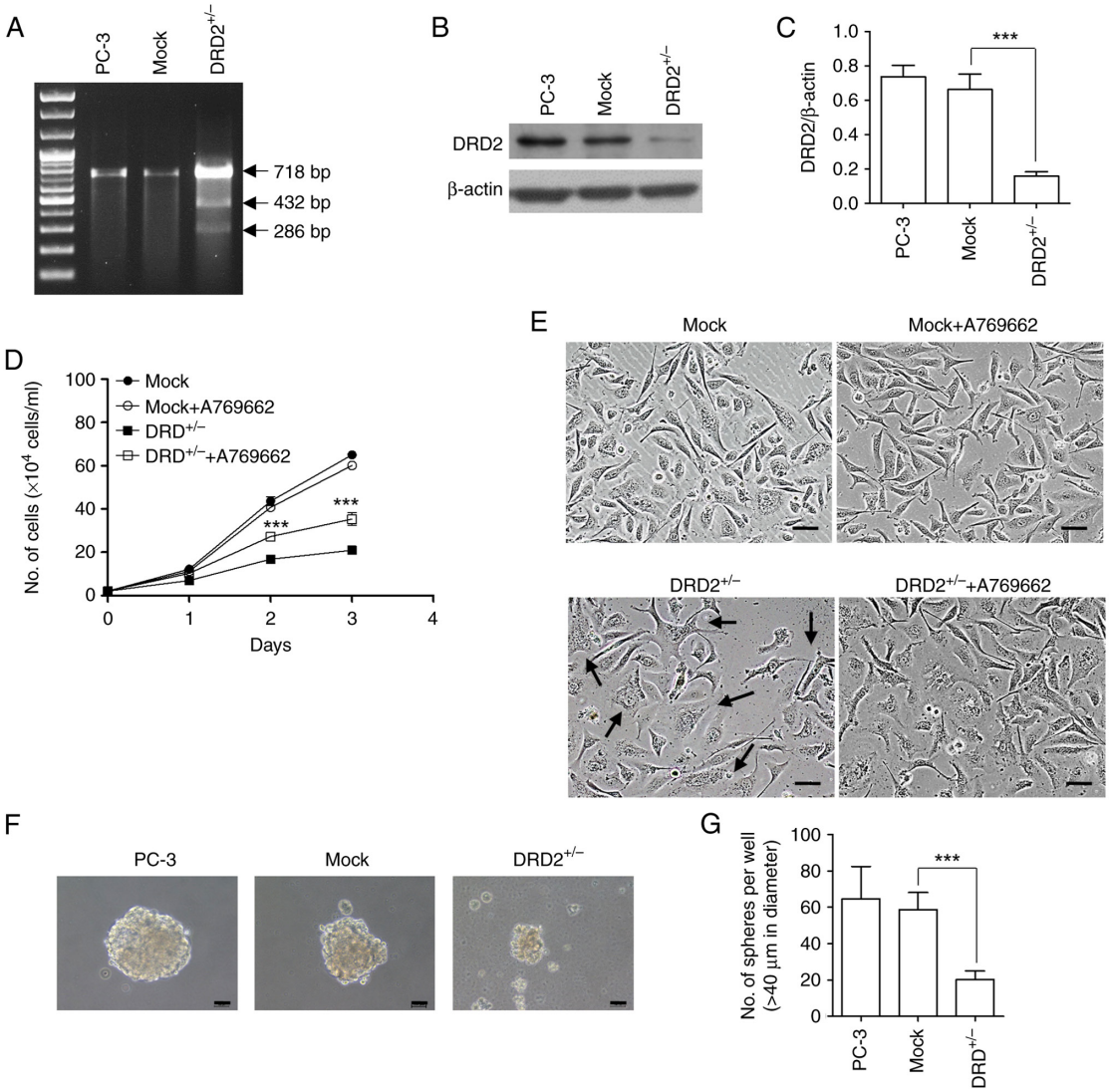

Figure 9. Changes in the characteristics of PC-3 cells following the heterozygous knockout of DRD2. (A) Agarose gel electrophoresis of PCR products amplified using genomic DNA isolated from wild-type and all-in-one vector-transfected PC-3 cells. (B) Lysates of wild-type, mock-transfected, and DRD2$^{+/-}$ PC-3 cells were subjected to western blotting to measure DRD2 protein expression. (C) Band densities of western blot images (n=3) were measured using ImageJ software. (D and E) Mock-transfected PC-3 cells and DRD2$^{+/-}$ PC-3 cells seeded at a density of 0.8x10^4 cells/ml in a 6-well plate were incubated for 3 days in the presence and absence of 30 μM A769662 and the number of cells were counted at the indicated times. Images of the cells were taken at the end of the experiments. Black arrows indicate cells whose morphologies are changed. Scale bar: 100 μm. Data are presented as mean ± SD (n=4). ***P<0.001 vs. DRD2$^{+/-}$. (F) Spheres formed from wild-type, mock-transfected, and DRD2$^{+/-}$ PC-3 cells in an ultralow attachment six-well plate for 10 days, Scale bar: 100 μm. (G) Round cell clusters larger than 40 μm in diameter were counted. Data are presented as mean ± SD (n=3). ***P<0.001 vs. Mock. DRD, dopamine receptor; AMPK, 5' AMP-activated protein kinase; mTOR, mammalian target of rapamycin; CSC, cancer stem cell; p-, phosphorylated.

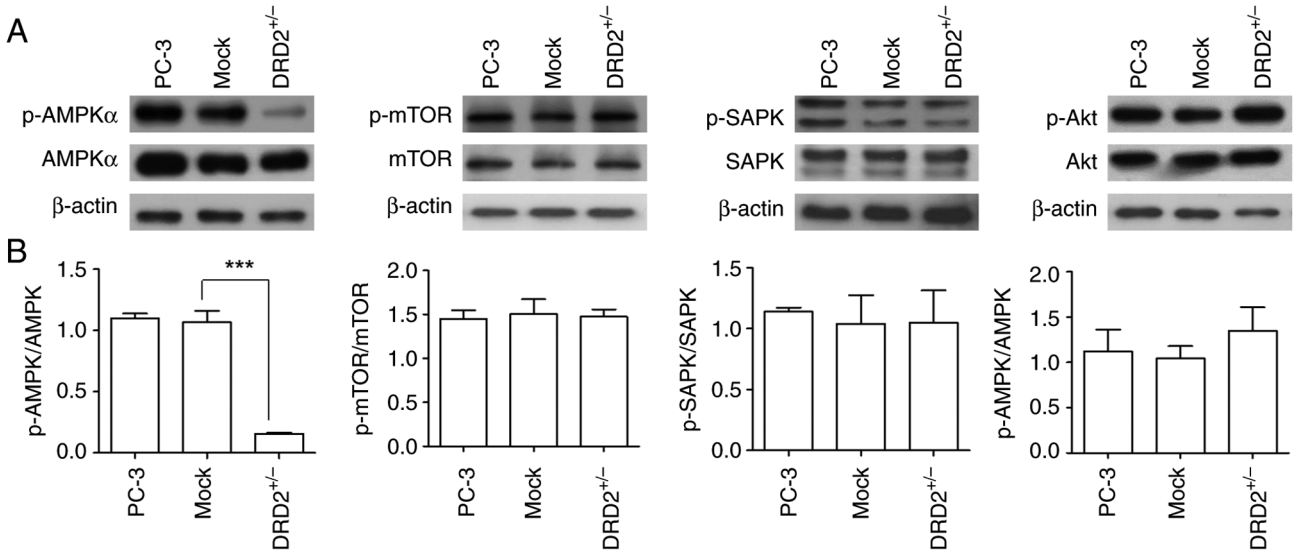

Figure 10. Suppressed phosphorylation of AMPK in DRD2$^{+/-}$ PC-3 cells. (A) Lysates of wild-type, mock-transfected, and DRD2$^{+/-}$ PC-3 cells were subjected to western blotting to measure the extent of AMPK phosphorylation. (B) Band densities of western blot images (n=3) were measured using ImageJ software. Data are presented as mean ± SD (n=3). ***P<0.001 vs. Mock. DRD, dopamine receptor; AMPK, 5' AMP-activated protein kinase; mTOR, mammalian target of rapamycin; SAPK, stress-activated protein kinase; p-, phosphorylated.

transduction pathways, including AMPK, was examined. As shown in Fig. 10, AMPK phosphorylation in DRD2$^{+/-}$ PC-3 cells was substantially decreased compared with that in the parental and mock-transfected PC-3 cells, whereas there were no significant differences in mTOR, SAPK/JNK, and Akt phosphorylation in the parental, mock-transfected, and DRD2$^{+/-}$ PC-3 cells, indicating that AMPK activity or phosphorylation is crucial for maintaining or inducing CSC properties.

Discussion

With the global increase in the incidence of prostate cancer, the number of patients with intractable prostate cancer, such as CRPC, is also rising. Various alterations, including the loss of normal androgen receptor expression in prostate carcinomas, are reportedly involved in the recurrence of prostate cancer and the acquisition of metastatic ability by carcinomas to other tissues, such as bones. CSCs have been reported to be crucial in these malignant processes (6). Our previous study using PC-3-derived CSC-like cells semiquantitatively determined the relative mRNA expression levels of five DR subtypes without providing information about their protein expression (17). There have been reports regarding the protein expression of some of the DR subtypes in carcinoma (10,24,25); however, to the best of our knowledge, there have been no reports regarding the protein expression of all five DR subtypes in CSCs or CSC-like cells. Because the immunocytochemistry methods used in this study were not quantitative, we could not compare the relative expression levels of the DR subtypes in the cells. Furthermore, the stained images of DRD3 were particularly difficult to obtain compared with those of the other subtypes in both the cell types.

L-741,626, a DRD2 antagonist, induced significant changes in the morphology of PC-3-derived CSC-like cells and the expression of pluripotency markers, including Oct4, Klf-4, and c-Myc. The DRD4 antagonist PD 168568 produced weak but similar results to those obtained using L-741,626. These results further confirm our previous results obtained with siRNA specific for the DR subtypes (17) and indicate that DRD2 and DRD4 coupled with G_i protein are involved in the maintenance of the properties of prostate CSC-like cells. Thus, in addition to studies on DRD2 and CSCs, further studies on the relationship between DRD4 and CSCs are required to understand the effect of dopamine receptors on the properties of CSCs. A previous study reported that DRD4 inhibition could be an effective tool for controling the properties of glioblastoma stem cells although it was not conducted using prostate CSCs (26). Our ongoing study using DRD4$^{+/-}$ or DRD4$^{-/-}$ is expected to provide a clearer understanding of the role of DRD4 in PC-3-derived CSC-like cells. The *in vivo* study that examined the antitumor effect of L-741,626, which exhibits stronger *in vitro* effects than PD 168568, indicated that a specific DRD2 antagonist could be used as an antiprostate cancer agent. However, even if a safe and effective DRD2 antagonist against CPRC is discovered, combination therapy with conventional therapeutic agents, such as cytotoxic and androgen-targeted agents, is required because a tumor contains a heterogeneous population of differentiated carcinomas in addition to CSCs (11).

Five different types of siRNA specific to each DR subtype were used to confirm whether the effects of specific antagonists against the subtypes effectively downregulated the expression of the mRNA corresponding to each DR subtype. The downregulation of the mRNA of the DR subtypes produced opposite effects to those expected from the intrinsic functions of the DR subtypes on adenylyl cyclase (23). While the downregulation of DRD2, DRD3, and DRD4 (G_i protein coupled receptors) appeared to inhibit adenylyl cyclase in the cells, that of DRD1 and DRD5 (G_s protein coupled receptors) appeared to cause the cells to lose their ability to activate adenylyl cyclase. These experiments were designed to validate whether the downregulation of DR subtypes caused by siRNA transfected into

cells was effective. However, further studies are warranted to determine whether fluctuations in cAMP concentrations induced by DRD2 and DRD4 inhibition are related to changes in the properties of PC-3-derived CSC-like cells. Nevertheless, obtaining an answer is difficult because DRD3 downregulation did not cause clear changes in the morphology, growth, and invasion ability of PC-3-derived CSC-like cells, although it induced an increase in the cAMP concentration.

As shown in our previous study (17), which revealed the inhibition of AMPK phosphorylation by thioridazine in PC-3-derived CSC-like cells, siRNA specific for DRD2 substantially inhibited AMPK phosphorylation in PC-3-derived CSC-like cells, further confirming that DRD2 inhibition leads to the loss of PC-3-derived CSC-like cell properties via AMPK inhibition. To determine whether the lack of DRD2 itself affects the formation of CSC-like cells and the regulation of AMPK phosphorylation, we attempted to prepare DRD2 homozygous null ($DRD2^{-/-}$) PC-3 cells without success. Complete DRD2 knockout appeared to cause the $DRD2^{-/-}$ cells to lose their proliferative ability, making the cloning of $DRD2^{-/-}$ cells impossible (Data not shown here, but our ongoing study also failed to obtain $DRD2^{-/-}$ DU 145 human prostate carcinomas). Although we cannot conclusively state that the presence of DRD2 is essential for the proliferation or survival of all types of carcinoma cells because we have not yet found other studies that have prepared and used $DRD2^{-/-}$ carcinoma cells, DRD2 appears to be important for the proliferation or survival of certain types of prostate carcinoma cells. Thus, instead of $DRD2^{-/-}$ cells, heterozygous null ($DRD2^{+/-}$) PC-3 cells were prepared and subjected to further study. The reduced expression of DRD2 protein in $DRD2^{+/-}$ PC-3 cells correlated well with reduced growth rates, changes in morphology, and reduced sphere formation capacity. The fact that A769662, an AMPK activator, partially restored the growth of $DRD2^{+/-}$ PC-3 cells suggests that the decreased AMPK activity induced by the heterozygous knockdown of $DRD2^{+/-}$ PC-3 was partially restored by A769662. Although the size and number of spheres formed from $DRD2^{+/-}$ PC-3 cells were smaller and fewer than those from $DRD2^{+/+}$ PC-3 cells, respectively, we attempted to prepare a monolayer culture of CSC-like cells using $DRD2^{+/-}$ spheres to investigate the effects of reduced DRD2 expression on signal transduction in PC-3-derived CSC-like cells. However, this approach was unsuccessful because the growth rate of single cells prepared from the $DRD2^{+/-}$ spheres was too low to form a monolayer culture. Thus, we used $DRD2^{+/-}$ PC-3 cells instead of using $DRD2^{+/-}$ CSC-like cells to examine changes in signal transduction induced by reduced DRD2 expression. The formation of spheroid carcinoma cultures is a well-known method for enriching CSCs *in vitro* (27). Accordingly, the fact that $DR^{+/-}$ PC-3 cells exhibited a reduced ability to form spheroid cultures and that preparing a monolayer culture of CSC-like cells from $DRD2^{+/-}$ spheres was almost impossible indicate that the intact presence of DRD2 is crucial during the conversion process of parental PC-3 cells to CSC-like cells.

To determine whether a signal transduction molecule was affected by DRD2 suppression, changes in the phosphorylation of several signal transduction molecules, including AMPK, whose phosphorylation was decreased by siRNA specific for DRD2 in PC-3-derived CSC-like cells, were examined in $DRD2^{+/-}$ PC-3 cells. Consistent with the results obtained using siRNA specific for DRD2, the reduction in DRD2 expression in $DRD2^{+/-}$ PC-3 cells resulted in a drastic decrease in AMPK phosphorylation, further indicating that the inhibition of AMPK phosphorylation interferes with the maintenance of the intact properties of PC-3-derived CSC-like cells. The role of AMPK has been reported in various cancer types. However, it is difficult to define its role in one sentence because activated AMPK suppresses or activates cancer or CSCs depending on the cancer type or stage (28-30). A review on the role of AMPK in advanced stages of prostate cancer supported the hypothesis that a complex of activated AMPK and pyruvate kinase 2 (PKM2) participates in the upregulation of cancer stemness genes by Oct4 (30), supporting the results of this study. In addition, another of our previous studies showed that AMPK suppression in PC-3-derived CSC-like cells and various cancer types using AMPK2a siRNA caused a loss of the properties of these cells (31).

Overall, DRD2 inhibition with a specific antagonist, suppression of DRD2 expression by DRD2 siRNA, or the heterozygous knockout of DRD2 causes PC-3-derived CSC-like cells to lose their properties and inhibits the formation of PC-3-derived CSC-like cells, followed by the inhibition of the phosphorylation of AMPK, a putative downstream signaling molecule of DRD2. Finding ways to effectively modulate the interrelation between DRD2 and AMPK in PC-3-derived CSC-like cells will provide an opportunity to identify new drug targets that can be useful for treating at least some types of incurable prostate cancer wherein AMPK is constitutively or highly activated.

Acknowledgements

Not applicable.

Funding

This research was supported by grants [grant nos. NRF-2019R1F1A1061276 and NRF-2022R1A2C1012921 (to SKP) and grant no. NRF-2019R1A6A1A03031807 (to YB)] from the National Research Foundation (NRF) of the Republic of Korea and a Korea University Grant (to SKP).

Availability of data and materials

The data generated in the present study may be requested from the corresponding author.

Authors' contributions

JP, HJJ and WKJ contributed to study conception and performed the experiments of immunocytochemistry, siRNA transfection, *in vitro* cell invasion assay, preparation of DRD2 heterozygous knockout PC-3 cells, cAMP assay, RT-PCR and tumor xenograft assay. DYK performed western blotting. YLG and HJK performed cell growth assay and immunocyochemistry experiments. JSK and JWY contributed to the design of tumor xenograft assays and cellular signaling studies, and confirmed the authenticity of all the raw data. YB and SKP designed the study and wrote the manuscript. All authors read and approved the final version of the manuscript.

Ethics approval and consent to participate

The Korea University IACUC (protocol number: KUIACUC-2021-0028; Seoul, Republic of Korea) approved the animal experiments.

Patient consent for publication

Not applicable.

Competing interests

The authors declare that they have no competing interests.

References

1. Siegel RL, Miller KD, Wagle NS and Jemal A: Cancer statistics, 2023. CA Cancer J Clin 73: 17-48, 2023.
2. Komura K, Sweeney CJ, Inamoto T, Ibuki N, Azuma H and Kantoff PW: Current treatment strategies for advanced prostate cancer. Int J Urol 25: 220-231, 2018.
3. Sekhoacha M, Riet K, Motloung P, Gumenku L, Adegoke A and Mashele S: Prostate cancer review: Genetics, diagnosis, treatment options, and alternative approaches. Molecules 27: 5730, 2022.
4. Richardson GD, Robson CN, Lang SH, Neal DE, Maitland NJ and Collins AT: CD133, a novel marker for human prostatic epithelial stem cells. J Cell Sci 117: 3539-3545, 2004.
5. Collins AT, Berry PA, Hyde C, Stower MJ and Maitland NJ: Prospective identification of tumorigenic prostate cancer stem cells. Cancer Res 65: 10946-10951, 2005.
6. Verma P, Shukla N, Kumari S, Ansari MS, Gautam NK and Patel GK: Cancer stem cell in prostate cancer progression, metastasis and therapy resistance. Biochim Biophys Acta Rev Cancer 1878: 188887, 2023.
7. Gogola S, Rejzer M, Bahmad HF, Alloush F, Omarzai Y and Poppiti R: Anti-cancer stem-cell-targeted therapies in prostate cancer. Cancers (Basel) 15: 1621, 2023.
8. de Thé H: Differentiation therapy revisited. Nat Rev Cancer 18: 117-127, 2018.
9. Enane FO, Saunthararajah Y and Korc M: Differentiation therapy and the mechanisms that terminate cancer cell proliferation without harming normal cells. Cell Death Dis 9: 912, 2018.
10. Sachlos E, Risueño RM, Laronde S, Shapovalova Z, Lee JH, Russell J, Malig M, McNicol JD, Fiebig-Comyn A, Graham M, *et al*: Identification of drugs including a dopamine receptor antagonist that selectively target cancer stem cells. Cell 149: 1284-1297, 2012.
11. Rane JK, Pellacani D and Maitland NJ: Advanced prostate cancer-a case for adjuvant differentiation therapy. Nat Rev Urol 9: 595-602, 2012.
12. Pérez G, López-Moncada F, Indo S, Torres MJ, Castellón EA and Contreras HR: Knockdown of ZEB1 reverses cancer stem cell properties in prostate cancer cells. Oncol Rep 45: 58, 2021.
13. Lee Y, Yoon J, Ko D, Yu M, Lee S and Kim S: TMPRSS4 promotes cancer stem-like properties in prostate cancer cells through upregulation of SOX2 by SLUG and TWIST1. J Exp Clin Cancer Res 40: 372, 2021.
14. Jiang N, Ke B, Hjort-Jensen K, Iglesias-Gato D, Wang Z, Chang P, Zhao Y, Niu X, Wu T, Peng B, *et al*: YAP1 regulates prostate cancer stem cell-like characteristics to promote castration resistant growth. Oncotarget 8: 115054-115067, 2017.
15. Roney MSI and Park SK: Antipsychotic dopamine receptor antagonists, cancer, and cancer stem cells. Arch Pharm Res 41: 384-408, 2018.
16. Rosas-Cruz A, Salinas-Jazmín N and Velázquez MAV: Dopamine receptors in cancer: Are they valid therapeutic targets? Technol Cancer Res Treat 20: 15330338211027913, 2021.
17. Lee SI, Roney MSI, Park JH, Baek JY, Park J, Kim SK and Park SK: Dopamine receptor antagonists induce differentiation of PC-3 human prostate cancer cell-derived cancer stem cell-like cells. Prostate 79: 720-731, 2019.
18. Hill SJ and Young M: Antagonism of central histamine H1 receptors by antipsychotic drugs. Eur J Pharmacol 52: 397-399, 1978.
19. Johnson DE, Nedza FM, Spracklin DK, Ward KM, Schmidt AW, Iredale PA, Godek DM and Rollema H: The role of muscarinic receptor antagonism in antipsychotic-induced hippocampal acetylcholine release. Eur J Pharmacol 506: 209-219, 2005.
20. Richtand NM, Welge JA, Logue AD, Keck PE Jr, Strakowski SM and McNamara RK: Dopamine and serotonin receptor binding and antipsychotic efficacy. Neuropsychopharmacology 32: 1715-1726, 2007.
21. Jung HS, Lee SI, Kang SH, Wang JS, Yang EH, Jeon B, Myung J, Baek JY and Park SK: Monoclonal antibodies against autocrine motility factor suppress gastric cancer. Oncol Lett 13: 4925-4932, 2017.
22. Kang MR, Park SK, Lee CW, Cho IJ, Jo YN, Yang JW, Kim JA, Yun J, Lee KH, Kwon HJ, *et al*: Widdrol induces apoptosis via activation of AMP-activated protein kinase in colon cancer cells. Oncol Rep 27: 1407-1412, 2012.
23. Beaulieu JM and Gainetdinov RR: The physiology, signaling, and pharmacology of dopamine receptors. Pharmacol Rev 63: 182-217, 2011.
24. Prabhu VV, Madhukar NS, Gilvary C, Kline CLB, Oster S, El-Deiry WS, Elemento O, Doherty F, VanEngelenburg A, Durrant J, *et al*: Dopamine receptor D5 is a modulator of tumor response to dopamine receptor D2 antagonism. Clin Cancer Res 25: 2305-2313, 2019.
25. Rosas-Cruz A, Salinas-Jazmín N, Valdés-Rives A and Velasco-Velázquez MA: DRD1 and DRD4 are differentially expressed in breast tumors and breast cancer stem cells: Pharmacological implications. Transl Cancer Res 11: 3941-3950, 2022.
26. Dolma S, Selvadurai HJ, Lan X, Lee L, Kushida M, Voisin V, Whetstone H, So M, Aviv T, Park N, *et al*: Inhibition of dopamine receptor D4 impedes autophagic flux, proliferation, and survival of glioblastoma stem cells. Cancer Cell 29: 859-873, 2016.
27. Bahmad HF, Cheaito K, Chalhoub RM, Hadadeh O, Monzer A, Ballout F, El-Hajj A, Mukherji D, Liu YN, Daoud G and Abou-Kheir W: Sphere-formation assay: Three-dimensional in vitro culturing of prostate cancer stem/progenitor sphere-forming cells. Front Oncol 8: 347, 2018.
28. Hardie DG: Molecular pathways: Is AMPK a friend or a foe in cancer? Clin Cancer Res 21: 3836-3840, 2015.
29. Bonini MG and Gantner BN: The multifaceted activities of AMPK in tumor progression-why the 'one size fits all' definition does not fit at all? IUBMB Life 65: 889-896, 2013.
30. Gharibpoor F, Kamali Zonouzi S, Razi S and Rezaei N: AMPK's double-faced role in advanced stages of prostate cancer. Clin Transl Oncol 24: 2064-2073, 2022.
31. Kim TH, Park JH, Park J, Son DM, Baek JY, Jang HJ, Jung WK, Byun Y, Kim SK and Park SK: Stereospecific inhibition of AMPK by (R)-crizotinib induced changes to the morphology and properties of cancer and cancer stem cell-like cells. Eur J Pharmacol 911: 174525, 2021.